Neutral rare-gas containing charge-transfer molecules in solid matrices. III. HXeCN, HXeNC, and HKrCN in Kr and Xe

Mika Pettersson,[a] Jan Lundell, Leonid Khriachtchev, and Markku Räsänen
Laboratory of Physical Chemistry, P.O. Box 55, FIN-00014, University of Helsinki, Finland

(Received 10 February 1998; accepted 3 April 1998)

The synthesis of novel rare-gas compounds HXeCN, HXeNC, and HKrCN is reported. HKrCN represents the first stable compound with a Kr–C bond. The novel molecules are formed in solid Xe and Kr by first photolyzing monomeric HCN with a 193 nm ArF laser at 7.5 K. The photolysis produces isolated hydrogen atoms and CN radicals as evidenced by IR spectroscopy and laser induced fluorescence. Annealing of the Kr matrix at ~30 K and Xe matrix at ~50 K activates the hydrogen atoms, and they react with rare-gas atoms surrounding the CN radicals producing the rare-gas compounds, which are characterized in this work by means of IR spectroscopy and *ab initio* calculations. Other products observed are HNC and H_2CN. Infrared induced photochemical conversion of HXeNC to HXeCN is accomplished by exciting the Xe–H and C–N stretching fundamentals of HXeNC. The existence of low barrier between these two distinct isomers is confirmed by the *ab initio* calculations. © *1998 American Institute of Physics.* [S0021-9606(98)02826-8]

I. INTRODUCTION

Since the discovery of the first rare-gas compound by Bartlett *et al.* in 1962[1] a large number of such molecules has been synthesized.[2] Typically, these compounds contain a xenon–fluorine or xenon–oxygen bond, the other examples being rather rare. The first xenon–nitrogen bond in $FXeN(SO_2F)_2$ was reported in 1974 by DesMarteau and LeBlond and up to date this and a few similar compounds seem to be the only examples of Xe–N bonding.[3–6] In 1979, Turbini *et al.*[7] reported the synthesis of $Xe(CF_3)_2$ with a xenon–carbon bond but its unequivocal spectroscopic characterization is still lacking. During the last few years, a number of compounds with Xe–C bonds have been synthesized and characterized, including ionic compounds $(C_6F_5Xe)^+(C_6F_5BF_3)^-$, and $(R–C{\equiv}C–Xe)^+ BF_4^-$.[8,9] Recently, Kötting *et al.* characterized an interesting charge-transfer complex between difluorovinylidene and Xe.[10] The first krypton–nitrogen bond was reported by Schrobilgen in 1988 in an ionic compound $(HCNKrF)^+(AsF_6)^-$.[11]

Quite recently, we have reported and characterized by means of matrix isolation infrared spectroscopy and *ab initio* calculations several novel rare-gas compounds with a number of new bonds, including HXeCl, HXeBr, HXeI, HKrCl, and XeH_2.[12,13] These molecules have in common an X–H-fragment (X=rare-gas atom), which is bound to an atom with a large electron affinity. The system is strongly polar, X–H having positive partial charge and the rest of the molecule having negative partial charge. These compounds show extremely intensive characteristic X–H stretching vibrations and they can be therefore easily detected by means of IR spectroscopy. They are formed from neutral atoms in a thermal reaction[14–17] and thus can be prepared from hydrogen halides by photodissociating the precursor and then thermally mobilizing the hydrogen atoms.

The halogen atoms should not be the only fragments, which could form this type of rare-gas compounds and the natural choice for new candidates are the pseudohalogens like CN, SH, OH, and NCO. We chose to first study HCN because CN has a large electron affinity (3.8 eV), HCN can be easily synthesized and photolyzed with an ArF excimer laser, and the CN fragment does not dissociate further with 193 nm radiation. Also, HCN (DCN) has been extensively studied in Ar, Kr, and Xe matrices, and the spectra of the monomers, dimers, and trimers are well characterized.[18,19]

In this paper we report the formation, infrared spectra, and *ab initio* calculations of three novel rare-gas compounds, HXeCN, HXeNC, and HKrCN, the latter apparently being the first compound with a krypton–carbon bond.

II. COMPUTATIONS

A. Computational details

The calculations were performed within the GAUSSIAN 94 package of computer codes.[20] Electron correlation was considered via Møller–Plesset second order perturbation theory (MP2). For the Kr-compounds also QCISD and CCSD(T) levels of theory were employed. Relativistic pseudopotentials (ECP) (including a spin–orbit potential) were used for Kr and Xe.[21,22] These ECPs include the *d*-subshell in the valence space resulting in 18 valence electrons. The basis sets were used in a decontracted form and are denoted as LJ18. For Xe the larger R18 basis set by Runeberg *et al.* was included in this study.[23,24] This basis set is a reoptimized LJ18 basis on Xe where *d*- and *f*-functions are added to Xe.[23] The standard 6-311++G(2*d*,2*p*) basis set was used for hydrogen, carbon, and nitrogen in conjunction with the LJ18 and R18 basis sets. The harmonic vibrational frequen-

[a]Electronic mail: mika.pettersson@csc.fi

TABLE I. Equilibrium structures, Mulliken charges, dipole moments, and electronic energies of linear HXeCN, HXeNC and the T-shaped transition state. The bond lengths are in Å.

	HXeCN		HXeNC		TS	
	MP2/LJ18	MP2/R18	MP2/LJ18	MP2/R18	MP2/LJ18	MP2/R18
r Xe–H	1.7070	1.7180	1.6588	1.6696	1.6481	1.6598
r Xe–C	2.3921	2.3707			2.7210	2.6843
r Xe–N			2.3422	2.3066	2.6068	2.5683
r C–N	1.1784	1.1793	1.1865	1.1887	1.1943	1.1970
q (H)	−0.203		−0.161		−0.116	
q (Xe)	0.847		0.880		0.873	
q (C)	−0.401		−0.295		−0.438	
q (N)	−0.242		−0.424		−0.319	
μ (D)	7.437		9.265		8.581	
E_{el} (hartrees)	−219.319077	−220.126172	−219.307382	−220.115244	−219.300526	−220.109146

cies on all levels were calculated numerically. The calculations were carried out on CRAY C94 and SGI Power Challenge supercomputers at the CSC-Center of Scientific Computing Ltd. (Espoo, Finland).

B. Computational results

1. HXeCN and HXeNC

Linear structures HXeCN and HXeNC were found to be stationary points on the potential energy surface of this system, HXeCN being the lowest energy form. The transition state between these forms was found to correspond to the T-shaped structure in which the Xe–H fragment is at the right angle to the C–N fragment pointing almost to the middle of the C–N bond. The transition state was confirmed by a frequency calculation, which yielded one imaginary frequency. The geometrical parameters and charge distributions of HXeCN, HXeNC, and the optimized transition state at different computational levels are presented in Table I. It is notable that the calculations give a shorter Xe–H bond length and also stronger charge separation between Xe–H and C–N fragments for HXeNC than for HXeCN.

The calculated harmonic vibrational wave numbers together with the intensities are collected in Table II. The shorter Xe–H bond length of HXeNC is reflected in the higher wave number for the Xe–H stretching vibration compared to HXeCN. According to the calculated intensities, Xe–H stretching is the strongest absorption for HXeCN, while both Xe–H and C–N stretchings are of nearly the same intensity for HXeNC.

The energetics of different forms constituted of H, CN, and Xe is presented in Table III. The xenon compounds HXeCN and HXeNC are found to be high energy species when compared to the HCN+Xe asymptote, but lower in energy than the H+Xe+CN asymptote. The calculated dissociation energy D_e of HCN is somewhat higher than the experimental value of 5.67 eV (Refs. 25–28) probably because the description of the free CN radical at the MP2-level is rather poor. Therefore, to estimate the dissociation energy of HXeCN to H+Xe+CN, we compare the calculated energy difference between HXeCN and HCN+Xe with the experimental D_e of HCN. The best estimate for the energetics is assumed to be at the MP2/R18-level giving an electronic energy difference of 4.24 eV between HXeCN and HCN+Xe. This value gives 1.43 eV for the D_e of HXeCN into H+Xe+CN. Interestingly, the barrier from HXeNC to HXeCN is below 0.2 eV, as estimated at the both levels of theory used, which means that already one quantum in Xe–H or C–N stretchings is energetically sufficient to convert HXeNC into HXeCN.

2. HKrCN and HKrNC

Similarly to the results on Xe, HKrCN, and HKrNC both were predicted to be stable forms by calculations, HKrCN

TABLE II. Calculated vibrational wave numbers (in cm^{-1}) and IR intensities (in km mol^{-1}) of HXeCN, HXeNC, and the transition state between the two stable structures. The bending vibrations of the linear molecules are doubly degenerate.

	HXeCN			HXeNC			TS	
	MP2/LJ18 Wave number	IR intensity	MP2/R18 Wave number	MP2/LJ18 Wave number	IR intensity	MP2/R18 Wave number	MP2/LJ18 Wave number	IR Intensity
CN str.	2053.8	17.2	2041.3	2108.7	344.7	2054.1	2112.2	494.2
Xe–H str.	1874.9	1286.0	1820.1	2010.5	517.4	1987.9	1939.6	132.0
H–Xe–CN bend	677.7	3.0	664.6	654.3	0.6	628.0	541.2	1.6
							542.2	4.8
Xe–CN str.	297.3	163.6	300.6	305.2	191.2	316.1	273.2	138.9
Xe–C–N/ Xe–N–C bend	160.8	0.0	153.6	80.9	0.1	78.6	−74.4	0.5

TABLE III. The calculated energetics of the H, Xe, and CN containing systems, values in eV.

	MP2/LJ18	MP2/R18
$(XeH)^+ + (CN)^-$	9.971	10.190
H+Xe+CN	6.380	6.381
HXeCN(TS)[a]	5.144	4.701
HXeNC	4.957	4.535
HXeCN	4.639	4.238
Xe+HCN	0.0	0.0

[a]The optimized transition state between HXeCN and HXeNC.

being lower in energy. For the krypton species, the quality of the calculations was improved by using QCISD and CCSD(T) levels of correlation, while the best basis set used was LJ18. The calculated parameters at different levels are presented in Table IV and the harmonic wave numbers are given in Table V. Again, we can see that calculations predict stronger charge separation and accordingly higher wave numbers of Kr–H stretching for HKrNC compared to HKrCN. The C–N and Kr–H stretching wave numbers and intensities are rather sensitive to the level used in the calculations especially for HKrCN. We can see that MP2 gives higher wave numbers for Kr–H stretching for HKrCN than QCISD and especially CCSD(T), which is the best level used in this study. This can be understood, because krypton compounds are more weakly bound than xenon compounds and the potential energy surface near the dissociation limit is not described accurately by MP2.

In the case of HKrCN, according to CCSD(T) wave numbers and QCISD intensities, one should see one very strong Kr–H stretching band in the mid-infrared region, other intensities being weak. For the less stable HKrNC form the calculations predict strong bands for both C–N and Kr–H stretchings as in the case of HXeNC. Table VI presents the energetics of the Kr containing compounds. It shows in particular that the calculated isomerization barrier from HKrNC to HKrCN is very low, only 0.066 eV at the CCSD(T)/LJ18 computational level. If we compare the barrier heights of HKrNC and HXeNC at the same MP2/LJ18 level we can see that the calculated HKrNC barrier is almost five times lower. This means that HKrNC seems to be rather unstable with respect to isomerization into HKrCN.

The best estimate for the dissociation energies of HKrCN and HKrNC can probably be obtained from the CCSD(T)/LJ18 energetics. This level gives the dissociation energy of HCN extremely well (theory 5.626 eV, experiment 5.673 eV), and therefore we assume that the calculations are reasonably good for the other values as well. From the calculated values we obtain 0.52 and 0.29 eV for the D_e of HKrCN and HKrNC with respect to dissociation into H+Kr+CN.

III. EXPERIMENT

A. Experimental details

HCN (DCN) was synthesized by degassing 50% water solution of H_2SO_4 (D_2SO_4, 96%–98% deuteration, Merck) and then freezing it by liquid nitrogen and dropping solid KCN (pro analysi, Merck) on the frozen acid. The air was then pumped off and the vessel was allowed to warm up gradually giving out a smooth stream of HCN (DCN), which was dried by P_2O_5 and trapped by liquid nitrogen, the whole system being under vacuum. This procedure yielded very pure HCN (DCN) as was confirmed by a FTIR gas analyser (GASMET, Temet Instruments OY, Finland).

The details of the matrix preparation are given elsewhere.[12,13] In short, the premixed gas was deposited onto a CsI window cooled by a closed cycle He cryostat (Air products, DE 202A) at 20–30 K. After deposition, the sample was cooled to 7.5 K and photolyzed. HCN/Xe and HCN/Kr ratios of 1/2000 and deposition temperatures of 30 K and 20 K for xenon and krypton, respectively, were found to produce practically monomeric samples, which was necessary to minimize the unwanted side products in photolysis. When preparing the deuterated matrices the vacuum line was treated with D_2O in order to minimize the deuterium exchange on the walls.

The IR spectra were measured with a Nicolet 60 SX FTIR spectrometer with a resolution of $1.0\,cm^{-1}$ or $0.25\,cm^{-1}$ averaging 200 or 500 scans using a MCT detector and a KBr beamsplitter. The photolysis was carried out by an excimer laser (ELI-76, Estonian Academy of Sciences) operated at 193 nm (ArF), the pulse energy being typically 20 mJ.

Excitation of CN radicals was achieved by using the

TABLE IV. Equilibrium structures, Mulliken charges, dipole moments, and electronic energies of linear HKrCN and HKrNC. The bond lengths are in Å.

	HKrCN			HKrNC		
	MP2/LJ18	QCISD/LJ18	CCSD(T)/LJ18	MP2/LJ18	QCISD/LJ18	CCSD(T)/LJ18
r H–Kr	1.4677	1.4708	1.4958	1.4128	1.4176	1.4257
r Kr–C	2.3422	2.3774	2.3570			
r Kr–N				2.3391	2.3538	2.3465
r C–N	1.1787	1.1658	1.1722	1.1863	1.1767	1.1822
q (H)	−0.209			−0.164		
q (Kr)	0.883			0.953		
q (C)	−0.482			−0.403		
q (N)	−0.192			−0.386		
μ (D)	9.102			11.519		
E_{el} (hartrees)	−270.2048352	−270.206098	−270.2273988	−270.195992	−270.199614	−270.218845

TABLE V. Calculated vibrational wave numbers (in cm^{-1}) and IR intensities (in km mol^{-1}) of HKrCN and HKrNC. The bending vibrations of the linear molecules are doubly degenerate.

	MP2/LJ18		QCISD/LJ18		CCSD(T)/LJ18
	Wave number	IR intensity	Wave number	IR Intensity	Wave number
HKrCN					
CN str.	2078.2	615.8	2191.5	0.1	2135.3
H–Kr str.	2010.6	1610.7	1989.8	2116.5	1780.9
H–Kr–CN bend	650.4	3.7	627.8	5.1	617.4
Kr–CN str.	247.8	211.9	245.1	173.5	251.7
Kr–C–N/Kr–N–C bend	156.2	1.9	152.9	1.6	160.3
HKrNC					
CN str.	2458.2	569.2	2398.8	636.3	2309.0
H–Kr str.	2016.6	232.7	2111.5	291.0	2065.8
H–Kr–CN bend	613.8	10.5	593.4	10.6	595.4
Kr–CN str.	266.8	173.8	268.6	155.1	269.1
Kr–C–N/Kr–N/C bend	50.1	1.4	64.9	2.1	67.5

second harmonic of radiation from an optical parametric oscillator (Continuum, OPO Sunlite) providing radiation with a typical pulse energy of 10 mJ, repetition rate of 10 Hz, and pulse duration of about 5 ns. The emission spectra were detected with a single UV-VIS monochromator (SPEX 270 M, resolution 0.3 nm) equipped with a gated ICCD camera (Princeton Instruments).

B. Experimental results

1. HCN/Xe

The C–H stretching and bending infrared absorptions of monomeric HCN in solid xenon (1/2000 ratio) are presented in Fig. 1(a). The dimer bands (at 3268, 3270, and 732 cm^{-1}) are very weak. The spectrum is very similar to the one reported by Abbate and Moore showing a well resolved site structure.[18]

In the gas phase, the ultraviolet absorption of HCN starts around 190 nm,[29] and it is expected to be red shifted in condensed rare-gases providing weak absorption of 193 nm radiation. 193 nm irradiation at 7.5 K leads to decomposition of HCN. Simultaneously, CN absorption appears and increases during irradiation. The IR-spectrum of CN radical in solid xenon is presented in Fig. 2(a) showing the well resolved rotational structure as was reported in emission by Schallmoser *et al.*[30] The *Q*-branch of CN at 2039.8 cm^{-1} is exactly at the same position as reported by Schallmoser *et al.* The rotational constant is about 1.6 cm^{-1}, which shows slight reduction from the gas phase value of 1.87 cm^{-1}.[27] CN absorption grows monotonically under irradiation indicating it to be stable under 193 nm photolysis. Another photolysis product is HNC as can be seen by comparing our infrared data with the results of Milligan and Jacox in the Ar matrix.[31] HNC grows first but starts to decay after some time showing that at least part of HCN is converted to HNC, which is then further photolyzed. Finally, Xe_2H^+ is produced in the photolysis, as evidenced by its characteristic infrared spectrum.[32]

When more concentrated matrices were photolyzed we observed that multimeric HCN decomposes faster than the monomer. Normally we avoided the multimeric matrices because of the complexity of the products both in photolysis and after annealing.

In Xe matrices, the production of isolated hydrogen atoms was proven by observing the well known luminescence from the radiative relaxation of the xenon–hydrogen exciplex at around 255 nm following the excitation at 193 nm.[33–36] We failed to observe any luminescence from the CN radicals when pumped with resonant light from the OPO

TABLE VI. The calculated energetics of H, Kr, and CN containing systems (in electron volts).

	MP2/LJ18	QCISD/LJ18	CCSD(T)/LJ18
$(KrH)^+ + (CN)^-$	10.339	10.308	10.259
H+Kr+CN	6.381	5.552	5.626
HKrCN(TS)[a]	5.505	5.484	5.401
HKrNC	5.466	5.408	5.335
HKrCN	5.225	5.233	5.102
Kr+HCN	0.0	0.0	0.0

[a]The optimized transition state between HKrCN and HKrNC.

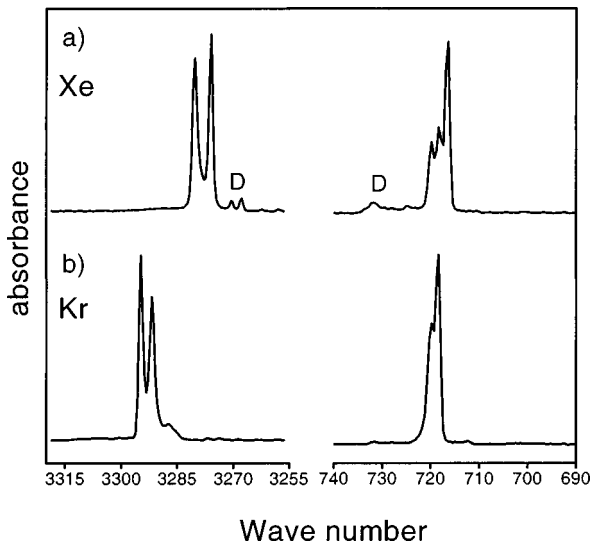

FIG. 1. The infrared absorptions of monomeric HCN in (a) Xe and (b) Kr matrices (at 7.5 K) in the C–H stretching and bending regions. The dimer bands are marked with D. The multiple peaks originate from site structure (see Ref. 18 for details).

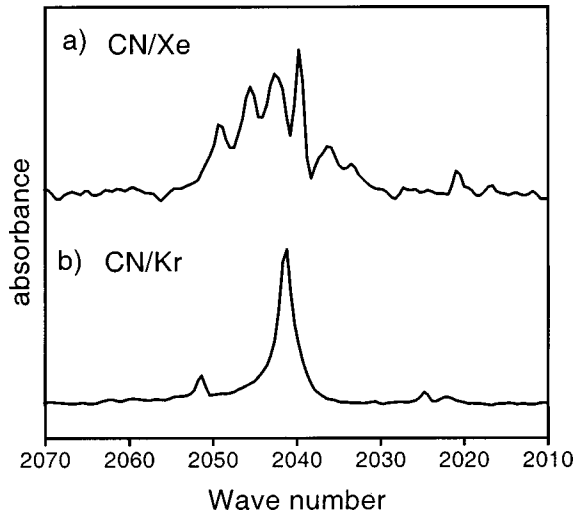

FIG. 2. The infrared absorptions of CN radical in (a) Xe and (b) Kr matrices at 7.5 K. In Xe, the rotational structure is clearly visible. CN radicals were produced by 193 nm photolysis of HCN.

around 400 nm corresponding to the $0\leftarrow 0$ transition of the $B\ ^2\Sigma\leftarrow X\ ^2\Sigma$ electronic transition[37,38] in agreement with the results of Bondybey *et al.*[39] indicating that the nonradiative relaxation channels dominate in solid xenon.

When photolyzed samples are annealed (up to 45–50 K), several strong absorptions appear and at the same time CN radicals decrease with a typical degree of decrease being 70% during annealing. The infrared spectrum of the partially deuterated sample after photolysis and annealing is presented in Fig. 3. The absorptions at 1166 and 1181 cm^{-1} are known to belong to XeH_2 and the corresponding deuterated species are also present.[13] The new absorptions are observed at 1623.8, 1851.0, and 2043.8 cm^{-1} and deuteration adds the bands at 1178.0 and 1338.8 cm^{-1}. The absorption at

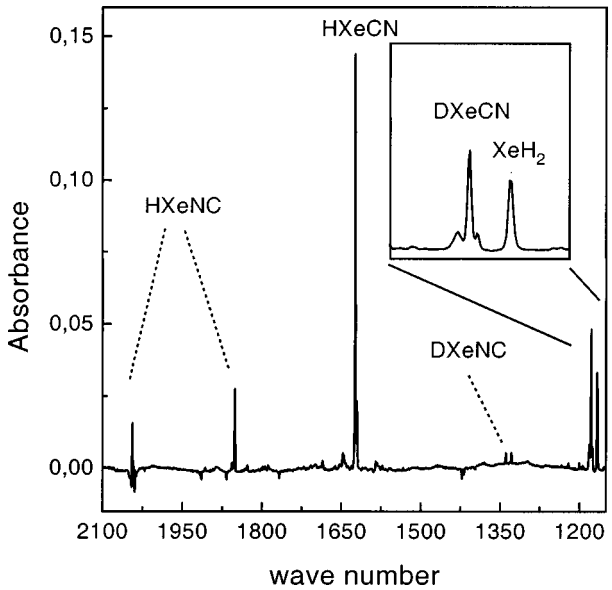

FIG. 3. The infrared absorptions appearing in annealing of the HCN (DCN)/Xe=1:2000-matrix after 193 nm photolysis. The figure was created by taking a difference spectrum between the situations after photolysis and after annealing to 55 K. The spectra are measured at 7.5 K.

TABLE VII. Observed product absorptions in HCN/DCN doped Xe and Kr matrices (7.5 K) photolyzed by 193 nm radiation and annealed to 50 K. The strongest absorptions are marked with an asterisk.

Xe(cm^{-1})	Kr(cm^{-1})	Assignment
477.0	478.2	HNC, bend
	618.0	HKrCN, bend
753.5		HXeD, Xe–D stretch
	882.8	HCNH?
	909.0	H_2CN, rock
	950.3	H_2CN, out-of-plane
1093.8		HXeD, Xe–H stretch
	1109.0	DKrCN, Kr–D stretch
	1217.9	HCNH?
1121.5		HXeD, Xe–H stretch
1166.0		XeH_2, antisymm. stretch
1175.7		DXeCN, Xe–D stretch
1178.0*		DXeCN, Xe–D stretch
1181.0		XeH_2, antisymm. stretch
1328.7	1332.7	H_2CN, scissors
1338.8		DXeNC, Xe–D stretch
	1490.8	HKrCN, Kr–H stretch
	1497.4*	HKrCN, Kr–H stretch
	1529 broad	HKrCN, Kr–H stretch
1620.4		HXeCN, Xe–H stretch
1623.8*	1650[a]	HXeCN, Xe–H stretch
1646 broad		HXeCN, Xe–H stretch
1851.0*	1878[a]	HXeNC, Xe–H stretch
1853.5		HXeNC, Xe–H stretch
2021.0	2024.7	HNC, C–N stretch
2033.4		CN $P2$
2036.3		CN $P1$
2039.8	2041.3	CN Q-branch
2042.6		CN $R0$
2042.3		HXeNC, N–C stretch
2043.8*	2048.5[a]	HXeNC, N–C stretch
2045.6		CN $R1$
2049.4		CN $R2$
3577.0	3598.6	HNC, H–N stretch

[a]HXeCN and HXeNC absorptions from a Kr matrix doped with 2% of Xe.

1623.8 cm^{-1} is assigned to HXeCN and the absorptions at 1851 and 2043.8 cm^{-1} to HXeNC. The 1178.0 and 1338.8 cm^{-1} peaks are assigned to DXeCN and DXeNC, respectively.

The rare-gas molecules are the main products in annealing, and the only other product observed is H_2CN.[40] The appearance of this molecule correlates nicely with the decrease of remaining HCN in annealing, indicating that hydrogen atoms react with HCN to form H_2CN. The IR absorptions of all the observed products are presented in Table VII.

Some studies on photolytic stabilities of HXeCN and HXeNC were carried out. In particular, HXeNC was found to photodissociate rapidly under 350 nm radiation, while HXeCN was completely stable. The most interesting results were obtained from the infrared irradiation experiments. When the sample containing HXeCN, HXeNC and the deuterated forms was irradiated for 28 h with a glowbar and a filter transmitting 3300–1200 cm^{-1} radiation, a conversion HXeNC (DXeNC)→HXeCN (DXeCN) was observed. When the process was repeated with a filter cutting wave numbers lower than 2150 cm^{-1} no similar changes were observed, indicating that the conversion was induced by pumping the fundamental vibrations of HXeNC (DXeNC).

2. HCN/Kr

The IR spectrum of HCN in Kr matrix is presented in Fig. 1(b) showing again monomeric trapping and good correspondence with the spectrum of Abbate and Moore.[18] HCN dissociates much less efficiently in Kr than in Xe, most probably because in Xe the threshold for absorption is shifted more to red and thus the absorption coefficient at 193 nm in Xe is larger than in Kr. It should be noted here that we did not observe any decomposition of HCN in Ar by 193 nm radiation.

The photolysis of HCN in Kr yields isolated CN radicals and HNC similarly to Xe. It is to be noted that no Kr_2H^+ was observed in monomeric matrices, and in the multimeric matrices, CN absorption was much weaker than in the monomeric matrices. Production of HNC in Kr is similar to Xe. It grows first, but starts to decrease after prolonged photolysis. The IR absorption of CN in Kr at 2041.3 cm^{-1} is presented in Fig. 2(b), and the position corresponds again exactly to that reported by Schallmoser *et al.* in emission,[30] but there is no observable rotational structure in our spectrum. We observe a single peak with a FWHH of 2.7 cm^{-1}, while the emission spectrum of Schallmoser *et al.* shows a broad structure with a FWHH of about 20 cm^{-1}. The production of CN radicals was confirmed by laser induced fluorescence. CN was excited by 389 nm radiation, which corresponds to the $(0\leftarrow 0)$ $B\ ^2\Sigma\leftarrow X\ ^2\Sigma$ transition[39] and $A\ ^2\Pi\rightarrow X\ ^2\Sigma$ luminescence was observed similarly to the lighter rare-gases.[37,41] Interestingly, we found that higher excited states of CN can be excited by 193 nm radiation, because the same emission spectrum was observed during the excimer laser photolysis.

Annealing of the HCN/Kr matrix after photolysis yields a strong absorption at 1497.4 cm^{-1} and a number of weaker absorptions, the relative intensity depending on the matrix history (monomeric vs multimeric, degree of dissociation of the precursor etc.). A typical IR spectrum is presented in Fig. 4. At the same time, CN absorption decreases typically by 40%, the rest being stable at temperatures used (<40 K). The generation of new absorptions starts around 25–30 K. A weak absorption at 618 cm^{-1} belongs to the same absorber than the 1497.4 cm^{-1} absorption, and this stronger peak shifts to 1109 cm^{-1} upon deuteration. These peaks are assigned to HKrCN (DKrCN). The strong peak is the Kr–H stretching and the weaker band is the H–Kr–C bending. We could not see any evidence for the formation of HKrNC. Other annealing products are H_2CN molecules, indicating again the reaction $HCN+H\rightarrow H_2CN$, which is supported by the decrease of HCN in annealing. It is important that neither in Kr nor in Xe growth for the precursor absorption was observed in annealing.

In Kr matrices, we also observed the growth of HNC during annealing, which is different from the situation in Xe where no growth of HNC was observed in a similar situation. Also absorptions at 883 and 1218 cm^{-1} were observed to appear. Similar absorptions were detected in Ar matrix by Jacox in the studies of reactions between HCN and H atoms.[40] These absorptions were assigned to HCNH, and the same assignment is possible in our case. All the relevant absorptions are collected in Table VII.

HKrCN can be slowly photolyzed by 389 nm radiation.

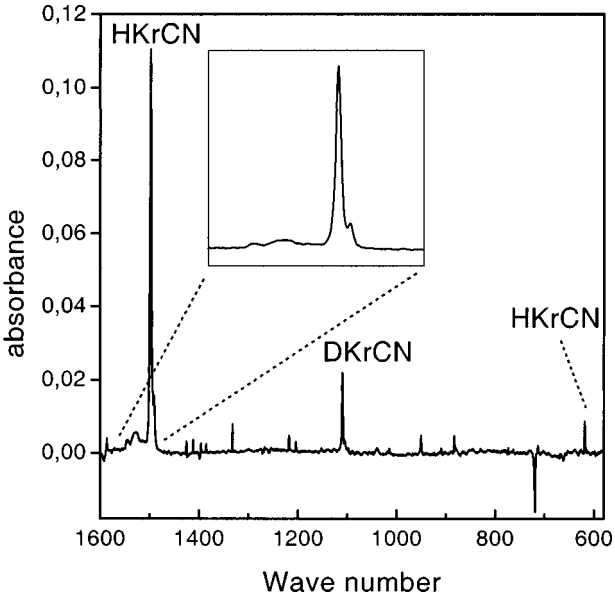

FIG. 4. The infrared absorptions appearing in annealing the HCN (DCN)/Kr=1:2000-matrix after 193 nm photolysis. The figure was created by taking a difference spectrum between the situations after photolysis and after annealing to 35 K. The spectra are measured at 7.5 K.

At the same time monomeric HCN increases. We cannot, however, exclude the possibility that other sources than HKrCN produce HCN under these conditions because there is also a slight decrease in H_2CN, HNC, and HCNH absorptions. Broadband glowbar radiation did not decompose HKrCN.

Finally, we made a HCN/Kr=1/2000 matrix, which was doped with 2% of Xe. The HKrCN absorption shifted slightly to 1495 cm^{-1}. Additionally, a new absorption appeared at 1650 cm^{-1}, which is assigned to HXeCN in solid krypton. Also, new absorptions at 1878 and 2048.5 cm^{-1} were assigned to HXeNC. All the absorptions are broader than in pure matrices.

IV. DISCUSSION

The assignment of the observed absorptions to the rare-gas molecules is justified on the basis of several facts. The spectra in xenon matrices are completely different from the spectra in krypton matrices, which suggests that Kr and Xe are constituents of the observed molecules. The presence of the rare-gas atoms in the compounds is confirmed by double doping experiment. The observations in this experiment are very similar to the case of HXeCl in Kr matrices.[12] The blue shifts of the xenon compounds in Kr can be explained by the smaller polarizability of solid krypton and the slight red shift of the Kr compounds by the presence of a small amount of more polarizable Xe atoms. Deuteration shows the presence of one hydrogen atom in each generated molecule. Moreover, the prepared matrices are monomeric with respect to HCN and in photolysis isolated CN radicals and hydrogen atoms are shown to be produced. Also, since the matrices contain very few reagents and in annealing only hydrogen atoms are mobilized the number of possible compounds generated in annealing is quite limited and we have no other candidates with similar spectroscopic properties to discuss.

The structure of the Xe–H stretching absorption band of HXeCN is very similar to the halogenated HXeY-species (Y=Cl, Br, I) showing a strong main peak and a broader side band at higher wave numbers and a sharp side peak at lower wave numbers.[12,14,42]

The calculated spectra of HXeCN and HXeNC are in good agreement with the observed except that the positions of Xe–H stretchings are overestimated. The numerical discrepancy can be explained partially by the harmonic approximation because the Xe–H stretchings should be rather anharmonic. Also we believe that the CCSD(T) level would give better agreement. In any case, the relative positions and especially the intensities of HXeCN and HXeNC are satisfactory. The infrared induced photoconversion of HXeNC to HXeCN finds the explanation in the calculated low barrier for this process.

In case of Kr, the calculations also overestimate the position of the Kr–H stretching band especially at the MP2-level but the agreement between theory and experiment becomes better at the higher levels of calculations. The CCSD(T)/LJ18 level seems to be satisfactory. It remains unclear at the moment, whether HKrNC is produced in experiments and then rapidly relaxed into HKrCN or into HNC+Kr, or it is generally unstable. In fact, if we estimate D_0 for HKrNC by assuming CN stretchings of the HKrNC and CN radical to be similar and use the calculated values for the rest of the vibrations of HKrNC in the harmonic approximation, we end up with a value of 0.06 eV for D_0 of HKrNC. Therefore, it seems probable that HKrNC cannot be considered a stable species at all.

It is interesting to discuss the similarity between the X–H stretchings of the CN and chlorine compounds. Both HXeCN, and HKrCN absorptions are within 25 cm^{-1} from the corresponding HXeCl and HKrCl absorptions, respectively. This is to be expected on the basis of the similar electron affinities of Cl and CN (3.6 vs 3.8 eV). The similar stretching wave numbers also indicate that the dissociation energies of the Cl and CN species are similar and normally the position of the X–H stretching can be considered as a good indicator of the stability of the molecule under study. On the other hand HXeNC seems to be an exception to this because it is higher in energy than HXeCN but it has a much higher Xe–H stretching wave number than HXeCN, and this can be due to the stronger charge separation in HXeNC as proposed by the calculations. In fact, there is a simple way of trying to explain the difference between HXeCN and HXeNC. The most dominant contribution to the stability of HXeY molecules (Y=fragment with a large electron affinity) is the ionic HX^+Y^- configuration. On the other hand, H^-X^+Y configuration should also be considered. The greater stability of HXeCN might be due to the significant contribution of the H^-Xe^+CN resonance structure in the total wave function of the system, while in HXeNC this contribution could be smaller. This idea explains the stronger partial negative charge of hydrogen in HXeCN compared to HXeNC, and also a smaller negative charge in the CN-fragment, and accordingly the difference in the Xe–H stretching wave number. The stretching wave number of the free XeH^+ at 2187 cm^{-1} (Ref. 43) can be considered as the upper limit for the wave number of the Xe–H stretching vibration for any HXeY compound and this value corresponds to full charge separation i.e. ion pair $(HXe)^+Y^-$. This limit is never quite reached in HXeY compounds. In addition, in solid xenon, the wave number should be red shifted to some extent because of the solid polarizable host. On this basis, HXeNC actually already has a very strong ion pair character, the strongest among all the HXY species observed so far.

It is important to emphasize that, especially in Xe, the rare-gas compounds are clearly the most dominant products after photolysis of the precursor and thermal mobilization of hydrogen atoms. Actually, the only other visible product is H_2CN, and it seems to be quite minor, indeed. This observation again shows that once the precursor is dissociated in the solid rare-gas environment, it can only recombine back via the potential energy surface of the corresponding rare-gas compound,[14] and in all the cases studied so far hydrogen atoms have been trapped extremely efficiently in the rare-gas compounds. Also in this work, no growth of the precursor was observed in annealing. The remaining question is whether hydrogen molecules are formed and/or to what extent. It seems that under annealing the formation of H_2 is prevented by the formation of XeH_2. This question is planned to be studied in our laboratory by Raman spectroscopy.

In solid krypton, other products are more visible, although the absorption of HKrCN is still clearly dominating the spectrum. Especially noticeable is the formation of HNC during annealing and the absence of HKrNC, and these two facts seem to be connected as follows. In solid Xe, if a hydrogen atom attacks the CN/Xe center (CN radical surrounded by xenon atoms) from the carbon side the reaction produces HXeCN and if a hydrogen atom attacks from the nitrogen end, the result is HXeNC. In the case of krypton, due to the possibility that HKrNC is not a stable molecule, if a hydrogen atom attacks the CN/Kr center from the nitrogen end, the resulting molecule is HNC. This idea explains the difference between Kr and Xe matrices. On the other hand, as was discussed previously, it is possible that HKrNC is formed but it relaxes fast either to HKrCN or HNC+Kr.

In our previous paper, we concluded that HXY-type compounds are formed from neutral atoms in a thermal reaction.[14] The results of this paper confirm the generality of this conclusion. As was mentioned earlier, in monomeric Kr matrices we observed no formation of ionic centers like Kr_2H^+. In Xe, the formation of Xe_2H^+ was observed in small amounts but it did not have any correlation with HXeCN and HXeNC. The stability of a part of CN radicals in annealing indicates that hydrogen atoms are thermally activated and the CN radicals are immobile.

In this work, the importance of monomeric trapping was noticed. When multimeric matrices were photolyzed the yield of CN radicals was dramatically reduced, and a number of additional absorptions appeared during photolysis and annealing. The yield of the rare-gas compounds subsequently remained low, and other products were enhanced. Also, if in monomeric matrices the photolysis was stopped when a large amount of the precursor was remaining the subsequent annealing produced less rare-gas molecules and more H_2CN.

V. CONCLUSIONS

The IR-spectra of three novel rare-gas compounds are reported including HXeCN, HXeNC, and HKrCN, the latter being the first observed stable compound with a krypton–carbon bond. HKrNC was not observed, and its stability is also computationally questionable. The formation of the molecules and the spectral assignments were confirmed by *ab initio* calculations. The isolated H and CN reagents are produced by trapping the monomeric HCN in rare-gas matrices after which the precursor is photolyzed by 193 nm radiation. After the photolysis, the matrices are annealed to activate the isolated hydrogen atoms and the rare-gas compounds are subsequently formed in a reaction of hydrogen atoms with CN/Xe or CN/Kr centers. A specific photo-induced conversion was observed from HXeNC to HXeCN. It was shown that HXeNC can be converted to HXeCN by exciting the fundamental vibrations of HXeNC by IR radiation.

The present observations correlate with the previous results obtained from the experiments with hydrogen halides and gives more indications that rare-gas molecules in general, and specifically HXY-type molecules with various atoms bound to the rare-gas atoms are possible to make. Also, as more krypton compounds are being found the preparation of the first argon compound become more and more realistic.

ACKNOWLEDGMENTS

W. Sander *et al.* are thanked for making their manuscript available before publishing. V. I. Feldman is thanked for many valuable discussions and for making his manuscript available before publishing.

[1] N. Bartlett, Proc. Chem. Soc. 218 (1962).
[2] See, for example, K. Seppelt and D. Lentz, Prog. Inorg. Chem. **29**, 167 (1982).
[3] R. D. LeBlond and D. D. DesMarteau, J. Chem. Soc., Chem. Commun. 555 (1974).
[4] D. D. DesMarteau, R. D. LeBlond, S. F. Hossain, and D. Nothe, J. Am. Chem. Soc. **103**, 7734 (1981).
[5] J. F. Sawyer, G. J. Schrobilgen, and S. J. Sutherland, J. Chem. Soc., Chem. Commun. 210 (1982).
[6] A. A. Emara and G. J. Schrobilgen, J. Chem. Soc., Chem. Commun. 1664 (1987).
[7] L. J. Turbini, R. E. Aikman, and R. J. Lagow, J. Am. Chem. Soc. **101**, 5834 (1979).
[8] G. H. J. Frohn and S. Jakobs, J. Chem. Soc., Chem. Commun. 625 (1989).
[9] V. V. Zhdankin, P. J. Stang, and N. S. Zefirov, J. Chem. Soc., Chem. Commun. 578 (1992).
[10] C. Kötting, W. Sander, J. Breidung, W. Thiel, M. Senzlober, and H. Bürger, J. Am. Chem. Soc. **120**, 219 (1998).
[11] G. J. Schrobilgen, J. Chem. Soc., Chem. Commun. 863 (1988).
[12] M. Pettersson, J. Lundell, and M. Räsänen, J. Chem. Phys. **102**, 6423 (1995).
[13] M. Pettersson, J. Lundell, and M. Räsänen, J. Chem. Phys. **103**, 205 (1995).
[14] M. Pettersson, J. Nieminen, L. Khriachtchev, and M. Räsänen, J. Chem. Phys. **107**, 8423 (1997).
[15] V. I. Feldman and F. F. Sukhov, Chem. Phys. Lett. **255**, 425 (1996).
[16] J. Eberlein and M. Creuzburg, J. Chem. Phys. **106**, 2188 (1997).
[17] V. I. Feldman, F. F. Sukhov, and A. Y. Orlov, Chem. Phys. Lett. **280**, 507 (1997).
[18] A. D. Abbate and C. B. Moore, J. Chem. Phys. **82**, 1255 (1985).
[19] K. Satoshi, M. Takayanagi, and M. Nakata, J. Mol. Struct. **413–414**, 365 (1997), and references therein.
[20] GAUSSIAN 94, Revision B.1, M. J. Frisch, G. W. Trucks, H. B. Schlegel, P. M. W. Gill, B. G. Johnson, M. A. Robb, J. R. Cheeseman, T. Keith, G. A. Petersson, J. A. Montgomery, K. Raghavachari, M. A. Al-Laham, V. G. Zakrzewski, J. V. Ortiz, J. B. Foresman, J. Cioslowski, B. B. Stefanov, A. Nanayakkara, M. Challacombe, C. Y. Peng, P. Y. Ayala, W. Chen, M. W. Wong, J. L. Andres, E. S. Replogle, R. Gomperts, R. L. Martin, D. J. Fox, J. S. Binkley, D. J. Defrees, J. Baker, J. P. Stewart, M. Head-Gordon, C. Gonzalez, and J. A. Pople, Gaussian, Inc., Pittsburgh, Pennsylvania, 1995.
[21] M. M. Hurley, L. F. Pacios, P. A. Christiansen, R. B. Ross, and W. C. Ermler, J. Chem. Phys. **84**, 6840 (1986).
[22] L. A. LaJohn, P. A. Christiansen, R. B. Ross, T. Atashroo, and W. C. Ermler, J. Chem. Phys. **87**, 2812 (1987).
[23] N. Runeberg, M. Seth, and P. Pyykkö, Chem. Phys. Lett. **246**, 239 (1995).
[24] N. Runeberg, Ph.D. thesis, University of Helsinki, 1996.
[25] D. Betowski, G. Mackay, J. Payzant, and D. Bohme, Can. J. Chem. **53**, 2365 (1975).
[26] J. Pacansky and G. V. Calder, J. Mol. Struct. **14**, 363 (1972).
[27] C. V. V. Prasad, P. F. Bernath, C. Frum, and R. Engelman, Jr., J. Mol. Spectrosc. **151**, 459 (1992).
[28] The value for the D_e was obtained by using the D_0 value (5.38 eV) from Ref. 25 and adding the zero point energies (ZPE) calculated from the fundamental absorptions of HCN and CN from Refs. 26 and 27. The harmonic approximation was assumed in the calculation of ZPE.
[29] H. Okabe, *Photochemistry of Small Molecules* (Wiley, New York, 1978).
[30] G. Schallmoser, A. Thoma, B. E. Wurfel, and V. E. Bondybey, Chem. Phys. Lett. **219**, 101 (1994).
[31] D. E. Milligan and M. E. Jacox, J. Chem. Phys. **47**, 278 (1966).
[32] H. Kunttu, J. Seetula, M. Räsänen, and V. A. Apkarian, J. Chem. Phys. **96**, 5630 (1992).
[33] M. Creuzburg, F. Koch, and F. Wittl, Chem. Phys. Lett. **156**, 387 (1989).
[34] M. Creuzburg and F. Wittl, J. Mol. Struct. **222**, 127 (1990).
[35] M. Kraas and P. Gürtler, Chem. Phys. Lett. **174**, 396 (1990).
[36] M. Kraas and P. Gürtler, Chem. Phys. Lett. **183**, 264 (1991).
[37] V. E. Bondybey, J. Chem. Phys. **66**, 995 (1977).
[38] A. Thoma, G. Schallmoser, A. M. Smith, B. E. Wurfel, and V. E. Bondybey, J. Chem. Phys. **100**, 5387 (1994).
[39] B. E. Wurfel, N. Caspary, J. Agreiter, A. Thoma, A. M. Smith, and V. E. Bondybey, J. Chem. Phys. **92**, 351 (1995).
[40] M. Jacox, J. Phys. Chem. **91**, 6595 (1987).
[41] H.-S. Lin, M. G. Erichson, Y. Lin, W. H. Basinger, and M. C. Heaven, Chem. Phys. **189**, 235 (1994).
[42] H. Kunttu and J. Seetula, Chem. Phys. **189**, 273 (1994).
[43] S. A. Rogers, C. R. Brazier, and P. F. Bernath, J. Chem. Phys. **87**, 159 (1987).